Geomorphology 211 (2014) 43–51

Contents lists available at ScienceDirect

Geomorphology

journal homepage: www.elsevier.com/locate/geomorph

A new sand-wedge–forming mechanism in an extra-arid area

Hongshou Li [a,b,*], Wanfu Wang [a,b], Fasi Wu [a,b], Hongtao Zhan [b], Guobing Zhang [a,b], Fei Qiu [b]

[a] The Conservation Institute of Dunhuang Academy, Dunhuang, 736200 Gansu, China
[b] National Research Centre for Conservation of Ancient Wall Paintings, Dunhuang, 736200 Gansu, China

ARTICLE INFO

Article history:
Received 10 September 2013
Received in revised form 26 December 2013
Accepted 27 December 2013
Available online 7 January 2014

Keywords:
Landmarks
The Mogao Grottoes
Polygon structures
Salts
Water

ABSTRACT

A survey found that sand wedges are widely distributed in the extremely extra-arid Gobi region of Dunhuang, China. The sand wedges are still developing. Well-developed sand wedges are surrounded by polygonal areas showing fractal structures. The depth of a well-developed sand wedge is 50–60 cm and its maximum width is 50–60 cm, so the depth/width ratio is 1.0. The interface between the wedge and matrix is arc-shaped. The mechanical composition of the sand wedges compared to the matrix is such that 76.72% of the particles have diameters ≤0.25 mm and show vertical sand laminations in the sand wedge, while 55.19% of the particles in the matrix are ≥2.00 mm in diameter. The particle diameters are consistent with the width of the sand-wedge fractures. The salt content in the sand wedges is 3.13 g/kg, while that of the matrix is 40.86 g/kg. The large salinity difference shows that the sand in the wedges comes from drift sand or cladding layers where salinity is lower, and that the sand wedge was formed in an arid climate. Displacement and pressure are closely associated with the daily temperature variation; they fluctuate significantly following the temperature. Measurements reveal the movement of thermal-contraction fissures. Pressure monitoring identified that wet expansions occurred after rainfall, which made the sand wedges become tightly joined to the matrix. Following this, as the soil became desiccated and shrank, a crack opened in the middle of the sand wedge. This was then filled with drift sand. With the next rainfall, the system moved into another development cycle. The current article reveals a new mechanism for forming sand wedges in extra-arid conditions. Arid sand wedges are a unique drought-induced surface landmark resulting from long-term, natural, dry-climate processes.

1. Introduction

Sand wedges are widely distributed in the cold tundra of high northern and southern latitudes near the poles (Black, 1976; Washburn, 1979; Andersland and Ladanyi, 1994; Marchant et al., 2002). Sand wedges are generally believed to be a result of chill-induced splits filling with sand, a process which repeats with the cycles of freezing and thawing year-by-year in frigid climates (Bockheim et al., 2009a,b). A sand wedge is one of the most important materials for paleoclimate reconstruction (Mears, 1981; Liang and Cheng, 1984; Wang and French, 1991; Murton, 1996; Adam et al., 2002; Murton and Bateman, 2007; Bateman et al., 2010).

When sand wedges were found to be widespread in mid-latitudes, the observation became important evidence in the judgment of the southern/northern edges of the periglacial regions in the late Pleistocene in the northern/southern hemispheres (French et al., 2003; Kovács et al., 2007). In China, sand wedges have been found in Daxinganling in northeastern China (Guo and Li, 1981), in the southern Ordos Plateau in Inner Mongolia (Dong et al., 1985, 1996; Cui et al., 2004), in the Datong Basin of Shanxi Province in northern China (Yang et al., 1983), in the Hexi Corridor area (Cui and Song, 1992; Wu et al., 2007), and the 'Third Pole' in northwestern China, as the Tibetan Plateau is often called (Guo, 1979; Pan and Chen, 1997; Shi et al., 1997; Chang et al., 2011). Where sand wedges have been found, they are generally thought to belong to the places where the periglacial southern edge existed in the late Pleistocene.

Along with the fact that sand wedges have been found in low latitudes near equatorial areas of Australia and northern Africa (Deynoux, 1982; Williams and Tonkin, 1985; Sohl et al., 1999), such observations are seen as key evidence in favor of the Snowball Earth hypothesis (Williams, 1975, 2001).

In order to more exactly reconstruct paleoclimate using sand-wedge data, the latter's formation mechanisms and formation conditions have been studied using dynamics (Lachenbruch, 1962), mechanics (Kaplar, 1963; Rist et al., 1999), model experiments (Li and Yang, 2000; Adam et al., 2002), electromagnetic induction (Singleton et al., 2010), paleodosing (D_e) (Bateman et al., 2010), etc. The temperature of formation of sand wedges has been tested by Romanovsky in the Siberian tundra, which is used as the basis for reconstructing paleoclimate (Wang et al., 2001, 2003). Bockheim et al. (2009a,b) believe that the sand wedges only form in Antarctica today when the mean annual air temperatures are −4 to −8 °C or colder. But Murton et al. (2000) advocate that care and caution are required in the use of ancient/relict primary sand-wedge data as quantitative paleoenvironmental indicators

* Corresponding author at: Dunhuang Academy, Dunhuang, Gansu Province 736200, China. Tel.: +86 937 8869046; fax: +86 937 8869103.
E-mail address: dhlhs69@163.com (H. Li).

0169-555X/$ – see front matter © 2014 Elsevier B.V. All rights reserved.
http://dx.doi.org/10.1016/j.geomorph.2013.12.028

because the modern active wedge distribution is still poorly known. Hence, they infer that the thermal climatic threshold values are questionable. We also think that all of these traditional studies are based on *wet* soil, which can freeze into ice as a precondition. In a periglacial climate, repeated freezing and thawing are the bases of sand-wedge formation. However, in recent years, we have found well-developed sand wedges in the dry Gobi Desert location of the famous Dunhuang Mogao Grottoes in China, where the climate has been in a state of drought since the last glacier disappeared (Liu, 2009). Further investigation found that sand wedges lurk in far-ranging locations in the Gobi Desert of the Dunhuang, which are developed to different levels and are still developing. Moreover, exploration has found that polygon vein structures exist on Mars as well as on Saturn's moon, Titan, and other planets (Mellon, 1997; Siebert and Kargel, 2001; Levy et al., 2009; Buczkowski et al., 2012). This suggests that other ways of forming such structures are possible apart from the freeze–thaw mechanism, i.e., other formation ways probably exist in extra-arid areas.

In addition, we found that deep-buried phreatic water evaporation occurs in extra-arid areas (Li et al., 2010a,b), and salt sources on the Gobi surface have been revealed. The salts come from deep underground as a result of groundwater migration — when the water evaporates, the salts are left in the soil and thus accumulate in the land's surface. They become a foundation material for a binder that is different from ice (Bockheim, 2007; Bockheim et al., 2009a,b). They can combine and consolidate loose gravel together and then, along with wet soil expansion and shrinking upon drying, form cracks.

Recently, soil researchers have made great progress in their field concerning expansion and contraction under alternating dry and wet conditions (Xiong et al., 2006; Huang and Shao, 2008). Shao and Lu (2003) presented a model to identify the relationship between a contracting feature index and the physical qualities of soil (Lu and Shao, 2003; Shao et al., 2007). A wet soil study indicated that lateral expansion occurs in wet sand soil (Luo and Fu, 2007). These studies have provided a new research platform for studying the formation of arid sand wedges. Thus, we suggest that sand wedges in extra-arid areas are formed by wet expansion when it rains and, following the polygon's dry shrinking, drift sands or surface sands entering into the cracks so developed. In this study, we describe and characterize sand-filled wedges and polygon matrices and propose a new descriptive model for their formation in extra-arid regions. Our proposals are based on detailed analyses of excavated sand wedges and rainfall experiments on wet expansion. By revealing the arid sand-wedge formation mechanism we hope to understand the historical landscape changes of the Mogao Grottoes and to provide a scientific basis for reasonable, accurate, and proper use of the unique landmarks formed by arid sand wedges.

2. Study areas

The city of Dunhuang is situated in the Eurasian heartland, at the Kumtag Desert fringe, where there are two modern alluvial fans (western and eastern). The Mogao Grottoes are located on the southern edge of the Dunhuang basin in the valley between the Sanwei and Mingsha mountains, in the Gansu Province of northwest China. The study areas are shown in Fig. 1. The main research region is a Gobi mesa located in the piedmont of Mingsha Mountain. It has an area of only about 10 km^2, and 0–60 cm of its depth is sand soil belonging to the Gobi

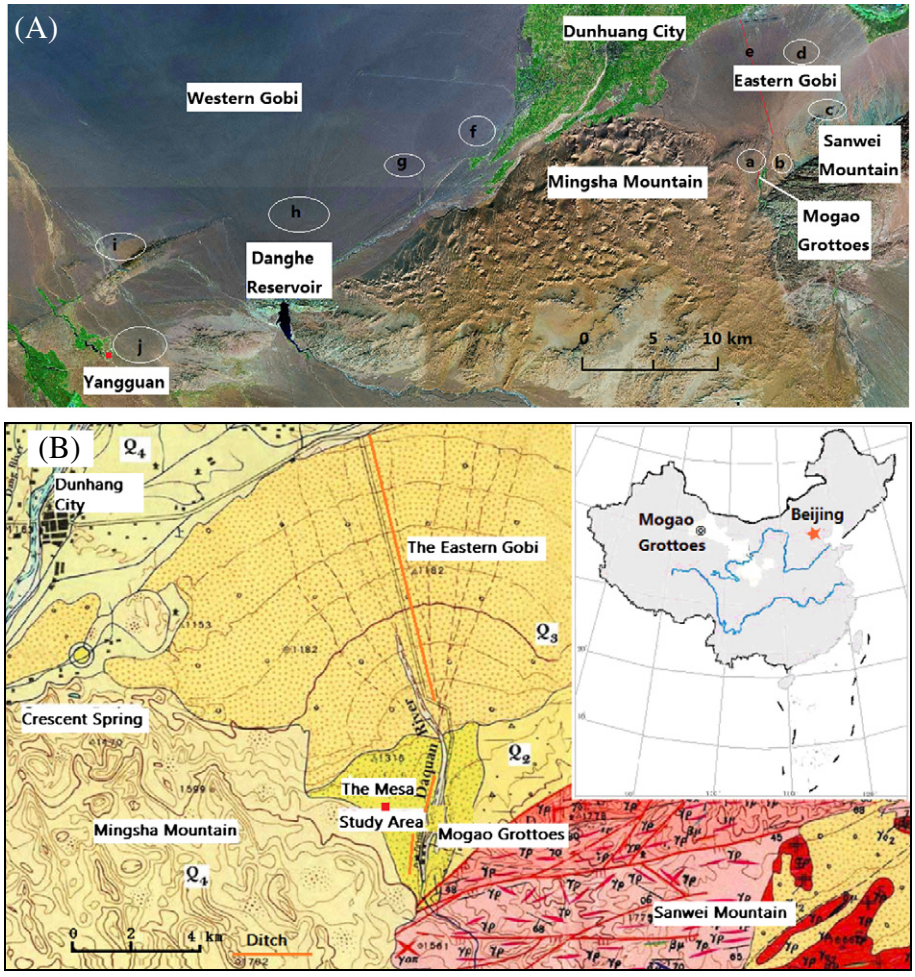

Fig. 1. The surveyed areas (A) and the geography around the Mogao Grottoes (B).

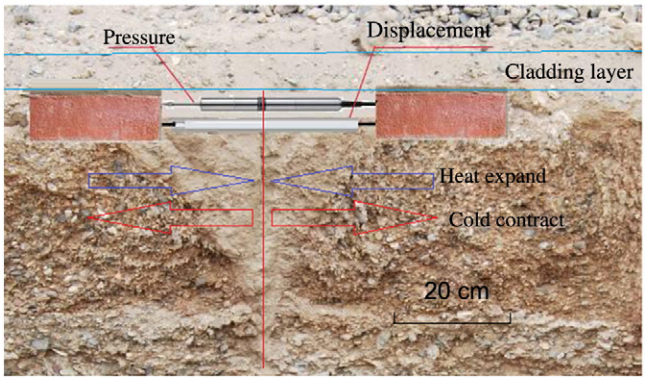

Fig. 2. Installation diagram of the JWYDC monitor and associated soil thermodynamics (made using Adobe Photoshop).

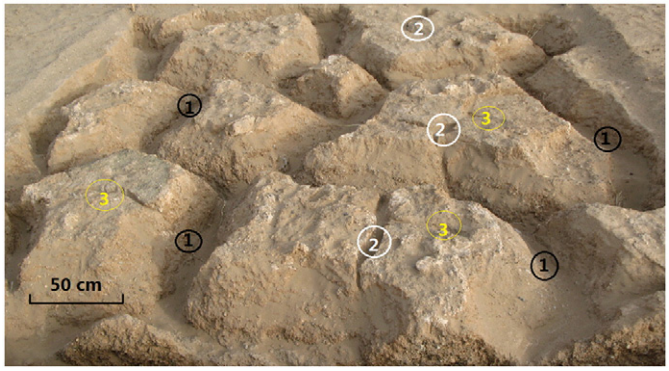

Fig. 3. The spatial structure of the sand-wedges' infilling in the 4 m × 4 m excavation. ① refers to the main sand-wedge filled space, ② refers to the secondary sand-wedge filled space, and ③ refers to the third grade sand-wedge filled space.

group of the Pleistocene (Q_3) (Guo et al., 2009). The sand wedge completely hides below the modern cladding layer (Wang et al., 2001, 2003), a surface layer, which has a thickness of about 3–5 cm. The climate is extremely dry. The average annual relative humidity is 31%, annual precipitation is 42.2 mm, potential evaporation is 4347.9 mm, and the annual average temperature is 11.3 °C. Climate records show that, since the weather station was established in 1937, the lowest recorded land surface temperature is −37.4 °C (15 Jan 1979). The solar radiation intensity is high. It can reach 1.1 kW/m^2, and the percentage of sunshine is 71%. The annual average wind speed is 4.1 m/s, and there prevails aeolian sand.

Based on the 'traditional' understanding of sand-wedge formation, if the sand wedges we have found in the extra-arid Dunhuang region are relicts of a late glacier, and if they were produced by wet soil freezing–thawing in cold conditions, then they should have stopped developing and have no developing sand wedges. Here we provide the evidence for development in many ways.

3. Methods

(i) Investigating the Gobi region is necessary around the Mogao Grottoes and the two modern alluvial fans west and east of Dunhuang City (Fig. 1). In the eastern Gobi we took advantage of underground cable laying in 2005. We investigated a 10-km ditch (1.4 m depth) and used the transect to get an idea of the morphometry and other characteristics of the sand wedge.

(ii) We selected a place on the top of Mogao Grottoes where the sand wedges are fully developed (location 'a' in Fig. 1, 40°02′13″ N., 94°47′38″ E.). We excavated a 4 m × 4 m area with typical representativeness and used archeological excavating methods (Paul, 1976; Macphail and Goldberg, 2010) to carefully study the particular characteristics of the sand wedges. The survey found that all of the sand-wedge's compositions, especially with respect to salt, have obvious differences from the matrix as a result of primary visual tests. This is a key clue to reveal the mechanism driving arid sand-wedge formation. So, after cleaning out the infill in the sand wedges, we measured the size and recorded the spatial structures of the sand wedges. At the same time, we sampled the infill and polygon matrices at 0, 5, 10, 20, 30, 40, 50, and 60 cm depths (1 cm thickness — we also sampled the drift sand nearby). We used particle size and the Udden–Wentworth grade scale to verify their mechanical composition. Water content was determined using an oven method, and the soluble-salt ion content was analyzed using a chromatographic analyzer (ICS-2500).

(iii) In order to obtain further evidence about whether the sand-wedge fissures are moving today, a displacement and pressure monitor (JWYDC) was installed. This was fixed in the sand wedge near the excavated 4 m × 4 m area, as shown in Fig. 2, and used to monitor the displacement, pressure, and temperature every 10 min. The results were analyzed using SPSS software to find the correlation between temperature, displacement, and pressure. Additionally, HOBO mini-monitors were installed in the matrix and the sand wedge at 10, 20, 30, and 40 cm. These were used to monitor the vertical temperatures every 10 min and analyzed for signs of vertical fracture activity.

(iv) Rainfall of 15 mm was simulated near the excavation point to measure potential wet expansion by monitoring the pressure and displacement using a JWYDC monitor. Meanwhile, we timely examined the infiltration depths through dug soil. During the monitoring period, a natural heavy rainfall event of 48.1 mm occurred on 12 June 2011, a once-in-a-century event here. After the rainfall, we covered a 10 m × 10 m area with plastic film to retain the water. The film was covered with 3 cm sand to guard against warming effects of the film. We observed the frozen status of the soil in winter and the salinity redistribution after one year to reveal the role of salts in sand-wedge formation.

4. Results and analysis

4.1. Survey results

On investigating the 10-km transect in the eastern Gobi (Fig. 1A, 'e'), small sand wedges were found under the modern alluvial surface. The depths of the wedges were about 50 cm, and the apparent widths of

Table 1
Characteristics and morphometry of the sand-wedges in different areas.

Survey areas (Fig. 1)	Width (cm)	Depth (cm)	Polygon width (cm)	Fractal grading	Development stage (developing or not)	Contains red-brown soil?
Gobi (d, e, f, g, h)	3–5	40–50	50–150	1	Initiation (developing)	No
Islands top (b, c)	20	40	120	2, 3	Development (developing)	Yes
Ancient riverbed (b, c)	0.5–1.5	40	50–120	1	Initiation (developing)	No
Yangguan (i, j)	30–40	40–50	50–150	3	Mature (third grade has stopped developing)	Yes
Mogao Mesa (a)	50–60	40–50	60–160	3	Mature (third grade has stopped developing)	Yes

Table 2
Grain size distribution (%) in a sand-wedge, matrix, and drift sand.

Position	Depth (cm)	Particle diameter (mm)								
		Clay <0.01	F.Sl. 0.01–0.05	C.Sl. 0.05–0.10	V.F.S. 0.10–0.25	F.S. 0.25–0.50	M.S. 0.5–1.0	C.S. 1.0–2.0	F.G. 2.0–10	M.G. 10–100
Surface	0	1.02	1.09	14.69	38.75	4.01	9.68	11.51	18.11	1.04
	5	0.81	1.15	15.09	57.17	5.68	7.28	4.85	7.83	0.16
Matrix	10	1.04	1.00	10.42	23.54	16.67	17.92	3.21	17.38	8.80
	20	2.50	1.10	10.78	16.82	9.78	17.31	6.04	26.37	9.29
	30	1.80	1.07	7.11	11.08	7.58	15.14	3.75	38.36	14.11
	40	1.34	1.30	4.81	6.62	4.05	11.49	3.70	42.07	24.61
	50	1.10	0.80	3.95	5.97	3.83	8.85	2.96	44.17	28.37
	60	0.74	0.69	3.32	6.60	3.56	5.70	1.77	22.75	54.86
Wedge	10	0.85	0.80	12.28	64.33	4.52	6.80	4.51	5.79	0.11
	20	0.84	0.88	16.30	63.20	2.48	6.24	4.22	5.76	0.10
	30	1.00	0.89	15.17	53.62	2.67	7.71	8.98	9.21	0.76
Drift sand	5	6.14	17.99	28.40	34.74	12.49	0.24	0	0	0

There were no particles with diameter >100 mm. Key: F.Sl. = fine slit; C.Sl. = coarse slit; V.F.S = very fine sand; F.S. = fine sand; M.S = medium sand; C.S. = coarse sand; F.G. = fine gravel; M.G. = medium gravel.

the wedges were 3–5 cm. The degree of development is slightly different in different areas, and in some sections only cracks exist and no sand wedges. Further investigation found well-developed sand wedges in the Gobi, e.g., the piedmont mesa, on top of the Mogao Grottoes (location 'a', Fig. 1A). In the east mesa (locations 'c' and 'd'), which should have sedimentation from the same period but has been eroded by the Daquan River and floods from the Sanwei Mountain, some relict islands have been left in the ancient riverbeds. The survey found that the sand wedges on top of the islands are larger. Its main wedge depth is 40 cm, the apparent width of the wedge is 20 cm, and the polygon matrix width is about 120 cm. However, from the top islands to the ancient riverbeds, the sizes of the sand wedges are significantly reduced. In the ancient riverbeds, the width of a wedge is only 1.0 cm. Also, they are filled with fresh drift sand, which is distinctly different from the surrounding sand; and the new infilling reaches to the surface. This indicates that the sand wedges in this area are still developing in situ.

A large-scale survey (Fig. 1A, locations 'a' to 'j') found that sand wedges with different degrees of development are distributed in the Dunhuang region from the eastern to the western Gobi. In western Gobi, the sand-wedge depth is about 40 cm and the apparent width of the wedge is 3–5 cm. We found that the older the diluvium, the larger the sand wedges. The degree of development of the sand wedges in the Yangguan piedmont mesa (locations 'i' and 'j') is similar to that in the Mogao Caves. Therefore, sand wedges in the extra-arid Gobi region are widespread.

The sand wedges have different degrees of development (stages of initiation, development, maturity). This is analogous to the chill-split sand wedges that formed in the edges of the periglacial region a long time ago (Brook et al., 1993; Bockheim et al., 2009a,b). Fully developed sand wedges are typically distributed on the mesa of Mogao. The characteristics of the sand wedges found in the survey are summarized in Table 1.

4.2. Sand-wedge characteristics

After cleaning out the infill from the excavated 4 m × 4 m square, the morphometrics of the sand wedges were determined, as shown in Fig. 3. The main sand-wedge depth is 50–60 cm, the width of the wedge mouth is also 50–60 cm (Table 1). Thus, the ratio of the depth/width (D/W) is 1.0. It has a V-shape, but the interface between the wedge body and matrix is arched (Fig. 2). In the irregular polygon matrix there are secondary sand wedges; their wedge depths are 20 cm, and their apparent widths are 5–10 cm. By careful observation, we also found more inferior sand wedges with depths and widths equal to 10 and 2.0 cm, respectively. The main sand wedge is filled with sand. However, the soil near the matrix is red-brown, which is the same as in the secondary- and third-grade sand wedges. Thus, this soil may have been filled in during the same early time period. The third-grade sand wedge is completely filled with the red-brown soil and has no sand infill at all. Thus, we infer that the third-grade sand wedges are not developing. We found that the structure and infilling of the sand wedges at Yangguan mesa are exactly the same as here. So, the sand wedges show a type of fractal structure (Cherykov, 2000). They are good examples of three-dimensional developing networks (Hallarire, 1989).

The mechanical compositions of the main sand wedge and matrix are shown in Table 2. In the sand wedge, 76.72% of the particles have a diameter ≤0.25 mm, similar to the surface layer (64.89% ≤0.25 mm) and drift sand (87.27% ≤0.25 mm; Table 2). However, 55.19% of the particles of the matrix have a diameter ≥2.00 mm. Obviously, the

Table 3
The contrast in the salt composition, salt content, and water content in the sand-wedges, matrix, and drift sand.

Position	Depth (cm)	Anion (g/kg)			Cation (g/kg)				Amount of ions (g/kg)	Water content (%)
		Cl^-	NO^{3-}	SO_4^{2-}	Na^+	K^+	Mg^{2+}	Ca^{2+}		
Surface	0	0.086	0.006	0.275	0.092	0.007	0.002	0.129	0.469	0.20
	5	0.020	0.002	0.076	0.038	0.007	0.001	0.027	0.143	0.21
Matrix	10	27.765	1.365	16.127	25.206	0.890	0.191	1.436	71.544	6.52
	20	8.840	0.672	15.626	13.095	0.370	0.099	0.678	38.701	7.38
	30	3.926	0.275	3.927	3.992	0.178	0.042	0.700	12.341	5.55
	40	1.917	0.083	1.966	1.766	0.097	0.012	0.548	5.842	3.37
	50	1.039	0.048	1.575	1.022	0.055	0.007	0.454	3.746	2.67
	60	0.907	0.046	1.331	0.928	0.059	0.007	0.352	3.277	1.79
Wedge	10	1.338	0.089	1.206	1.003	0.069	0.013	0.520	3.718	1.68
	20	0.767	0.055	1.427	0.799	0.049	0.008	0.430	3.105	1.26
	30	0.614	0.038	1.173	0.678	0.064	0.008	0.431	2.574	1.84
Drift sand	5	0.190	0.043	0.916	0.356	0.050	0.010	0.318	0.267	0.54

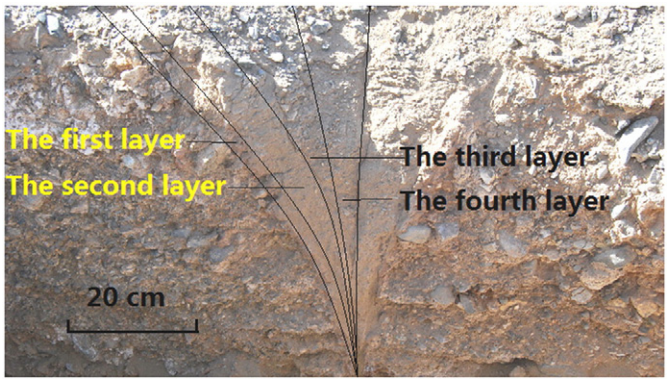

Fig. 4. The sand-wedge's vertical surface and the filling's lengthway layers in the excavated 4 m × 4 m area.

mechanical composition of the sand wedges is different from the matrix, in which gravel forms the level sediment layer. In the sand wedges, lengthway layers and V-shaped sand laminations are seen.

The salt components and salt and water contents in the main sand wedge and matrix are shown in Table 3. The salinity in the cladding layer is clearly lower than in the sublayers of the matrix and differs greatly in the matrix and sand wedge. At the same depth of 10–30 cm, the average salt content of the sand wedge is 3.13 g/kg; while in the matrix it is 40.86 g/kg, 13 times as high as in the sand wedge. The highest salinity of the matrices is at a depth of 10–20 cm, and here it is 16 times as great as in the corresponding part of the wedge. The water content distribution is consistent with the salinity distribution pattern — there exists combined water such as absorbed water, film water, and water of crystallization. As mirabilite is a representative salt in the Gobi soil, its water of crystallization leads to a water distribution similar to the salt distribution and higher in 10–20 cm (Li et al., 2011). The lower salinity in the sand wedges shows that the infill comes from drift sand (0.267%; Table 3) and the surface layer, i.e., the cladding layer, which has the lowest salt content. Moreover, the sand wedges cannot have experienced a wet climate period (Liu, 2009), otherwise the salts in the matrices would have dissolved and migrated to the sand wedges. This would lead to the salt content in the sand wedges being similar to that in the matrices. This supposition has been confirmed by testing the salinity of soil that had been covered by 10 m × 10 m plastic film after 48.1 mm of rainfall one year before. After one year of dissolved salt movement, the salt remained balanced so that the average salt content in the sand wedges was 36 g/kg. This is even higher than in the matrices (32 g/kg).

A distinct V-shaped, lengthway layer exists in the infilling in the sand wedges, as shown in Fig. 4. The textures of each layer are different from one another. The original level layers of matrices near the sand wedges have been curled upwards by the extrusion of the sand wedges (Fig. 2).

The sand wedges shown in Fig. 4 can be roughly sorted into four layers according to their particle diameters. The mechanical compositions of these layers are given in Table 4. The texture is obviously different in the different layers — the second layer is finer than the first, and the third is the coarsest one. Only 28% of the particles are more than 0.25 mm in size. This shows that in different periods the infilling material is different. Also, the particle size is closely related to the width of the fissure.

4.3. Monitoring of the sand-wedge fissures and temperature and analysis

The daily periodic change in the fissures in the sand wedges is shown in Fig. 5. The displacement increases with temperature rise, which means that the fissure size decreases when the temperature increases, and vice versa. The correlation coefficient between displacement and temperature was analyzed using SPSS software and found to be 0.62 ($P = 0.01$). The fissures of the sand wedges fluctuate with temperature; they are affected by the thermal expansion and contraction of the polygon structure (Fig. 2). The daily displacement of a fissure is 0–0.67 mm in the summer and 0–0.40 mm in the winter. The fissure is large enough to be filled by fine sand, and the moving mid-value is 0.20–0.38 mm, which coincides with the particle size (about 0.25 mm) of the main constituent of the fine sand wedges (Table 3).

The pressure behavior is similar to that of the displacement, it too changes with temperature and has daily fluctuations. The variation in the pressure over the same period is shown in Fig. 5. The correlation coefficient between pressure and temperature is 0.40 ($P = 0.01$).

As the daily temperature difference gradually decreases with depth (Fig. 6), the movement of the fissure is naturally like the letter 'V' (the upper part moves a large distance, and the lower part a small distance). This is one of the basic reasons why a sand wedge forms with a V-shape. The amount of contraction is linear with temperature and follows the basic formula for thermal expansion–contraction: $L = L_0(1 + a\,\Delta t)$. Here, L_0 is the initial length (when $\Delta t = 0$), Δt is the temperature difference, and a is the linear expansion coefficient that is characteristic of the material itself (Qin, 2011).

The yearly fracture activity is shown in Fig. 7. The whole of the displacement curve changes with yearly temperature, though the fluctuation range is small. The correlation coefficient is 0.23 ($P = 0.01$). In winter, the fissures become larger, and the yearly fluctuation range is more than 1.32 mm. Therefore, a few larger pieces of gravel are found in the sand wedges (Table 3).

As the soil is very dry in the extremely arid climate, the soil water only exists as bound water such as hygroscopic water and water of crystallization (Li et al., 2011). The freezing temperature of this water is very low. For instance, the freezing temperature of hygroscopic water is −78 °C (Zhu and Qian, 2005). Therefore, the conditions are not right for chill-induced splitting. Even in the plastic film covered area, where both sand wedges and matrices were kept wet, the ground did not freeze (this is an effect resulting from the high salt content) even in winter where the lowest temperature was −23 °C. Therefore, no fissures resulting from wet chill splitting are found in the Gobi Desert region of Dunhuang.

4.4. Rainfall and sand-wedge formation

Without rainfall, fissure activity itself does not necessarily mean that a sand wedge is forming. After the experiment simulating 15 mm rainfall, the monitored displacement, pressure, and temperature were as shown in Fig. 8A. At the 20th and 34th hour after watering, two abrupt

Table 4
Grain size distribution (%) in the lengthway layers in the sand-wedges.

Particle diameter (mm)	Clay <0.01	F.Sl. 0.01–0.05	C.Sl. 0.05–0.10	V.F.S. 0.10–0.25	F.S. 0.25–0.50	M.S. 0.5–1.0	C.S. 1.0–2.0	F.G. 2.0–10	M.G. 10–100
First layer	5.85	4.03	18.01	31.58	7.85	9.96	3.16	19.4	0.16
Second layer	1.40	4.90	10.09	62.23	12.75	4.40	1.88	2.36	0.00
Third layer	1.72	5.11	25.80	39.46	3.87	10.00	4.22	8.78	1.03
Fourth layer	1.02	4.01	39.20	36.58	2.80	7.34	1.97	6.38	0.70

There were no particles with diameter >100 mm. Key: F.Sl. = fine slit; C.Sl. = coarse slit; V.F.S = very fine sand; F.S. = fine sand; M.S = medium sand; C.S. = coarse sand; F.G. = fine gravel; M.G. = medium gravel.

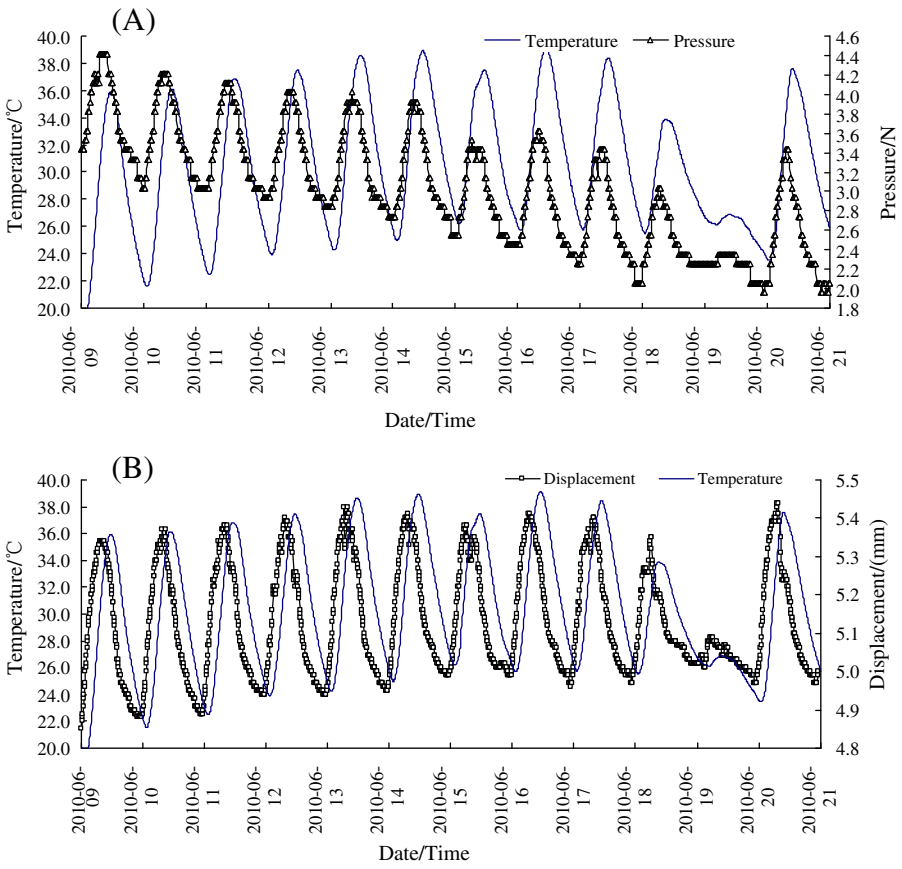

Fig. 5. The daily variations in the displacement and pressure with temperature.

pressure changes occurred (the pressuring times lasted 20–30 min). This clearly shows the existence of wet expansion processes.

After 48.1 mm of natural rainfall, abrupt pressure changes occurred many times, as shown in Fig. 8B. The characteristic appearance of abrupt pressure changes indicates that extrusion is not accomplished in one single action — rather, it is like an earthquake that has happened at the edge of a continental plate. Along the edge, depending on random local conditions, movement as the quake happens is discontinuous and action time is short. Here, if the soil water content has not reached a certain critical value, an abrupt pressure change will not happen. Certainly, monitoring shows that abrupt pressure changes will never occur if rainfall is absent. So, a wet expansion theory is identified by these experiments.

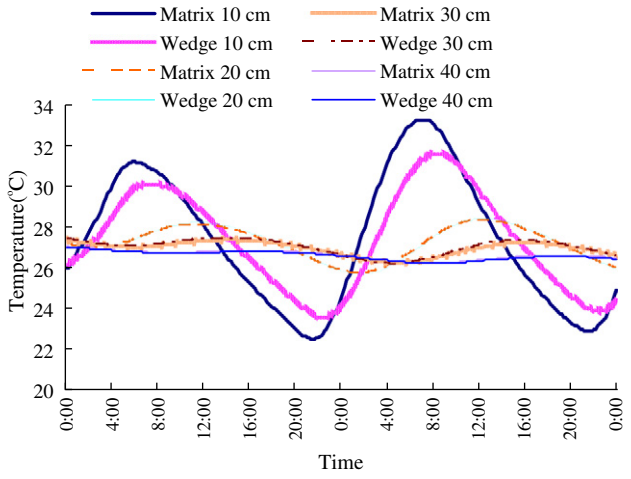

Fig. 6. The daily temperature changes at different depths in the sand-wedge and matrix.

After 15 mm of simulated rainfall, the infiltration depths in the sand wedges and the matrices were 25 and 10 cm, respectively, on the first day. On the second day they were 29 and 25 cm, respectively. After the third day, the infiltration depth in both sand wedges and matrices was close to 32 cm. Clearly, preferential infiltration occurs in the sand wedges after rainfall and, further, they absorb more water than the matrices.

The depth of the wet expansion is affected by the amount of rainfall and, furthermore, the width of the dry shrink fracture is also determined by it. Then, the fracture width will further determine the diameter of the particles in the sand wedges. Infilling in different historical periods is shown in Fig. 4. The diameter of the particles in the infill clearly reflects the historical fluctuations occurring in the alternating degree of dryness and wetness of the climate.

Generally, 85% of the rainfall events involve <5 mm of rain, so most of the rainwater is only absorbed by the cladding layer. Therefore, most rainfall cannot create wet expansion. Only if a rainfall event involves more than about 10 mm of rain is it sufficient to enable wet expansion. However, from local meteorological data, rainfall >10 mm at Mogao occurs less than once in every year. Therefore, we found many superimposed laminations on the upper fissure surface that were made by expansion after many small rainfall events, as shown in Fig. 9. This is another major reason why the wedge mouth develops more quickly than the under part. It is also why the sand wedge makes a curved shape along the matrix. When a large rainfall occurs, the sand wedge is completely wet and this produces enough pressure to make the superposed traces on the fissure surface straight and smooth.

Therefore, the sand wedges in extra-arid areas are formed by wet expansion and they are still developing. After the occurrence of the

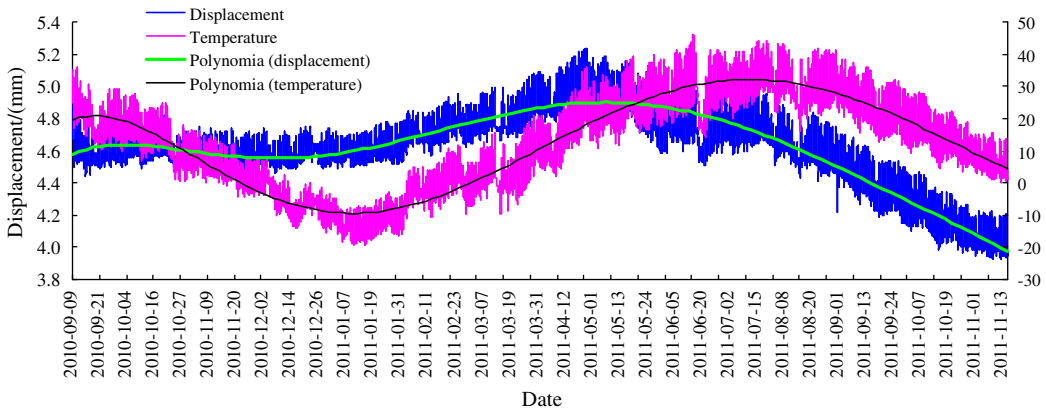

Fig. 7. Yearly changes in the sand-wedge fracture displacement and temperature.

processes of rainfall, water infiltration, wet expansion, dry shrinking, and sand filling, the sand wedge has finished a formation cycle. These cycles occur again and again with the rainfall in the extra-arid area and make the sand wedge develop continually.

5. Discussion

Although arid sand wedges have some characteristics similar to the freezing–thawing sand wedges in the tundra (such as fracture activity, V-shaped sand laminations, and the fact that they both obey the principle that heat bulges and cold shrinks) they also have some differences because of their different mechanisms of formation. These are discussed below.

Firstly, the arid sand wedges form in extra-arid backgrounds. The main combined materials are salts, which consolidate the loose gravels and come from phreatic water evaporation (Li et al., 2010b, 2011). Along with increasing salt content comes increasing connection strength between gravels, and this makes the matrices form larger polygon blocks. So, at last, a three-grade fractal structure is formed. In contrast, frozen sand wedges are formed in tundra or seasonally frozen ground (Murton et al., 2000) where conditions are mostly wet and frozen. They have higher moisture contents (the climate may be dry) and lower levels of salts (Bockheim, 2007). So, cracks are formed in the chilling climate and ice is the main combining material. But this does not mean that all high latitude sand wedges have formed simply by a wet freezing–thawing effect — arid sand wedges may also form in arid Polar regions.

Secondly, the depths of the sand wedges in extra-arid areas are different from the depths of frozen sand wedges. Soil temperature monitoring found that the deepest depth at which 0 °C is found is 60 cm in the Mogao Gobi, consistent with the depth of the sand wedges. This is shallower than the maximum frozen soil depth of 144 cm in the Dunhuang oasis in modern times. The key reason why frozen soil is deeper in the Dunhuang oasis is that in this location the frozen depth is based on wet soil and low salt content. If the soil becomes wet, the thermal conductivity increases, the temperature affected range will be enlarged, and the freezing depth will be deeper. Therefore, if the sand wedges were formed by freezing near late glaciers, a time in which it is generally believed that the temperatures were lower than in modern times, the depth of the sand wedges should be naturally deeper than 144 cm. However, our investigation has not found this to be the case. The frozen wedge depth is generally deeper than 2.0 m (Murton et al., 2000), and the D/W ratio of the sand wedge is more than 1.5 (Adam et al., 2002), which is greater than those in the Mogao ($D/W = 1.0$). This indicates that the sand wedges in this area are formed through

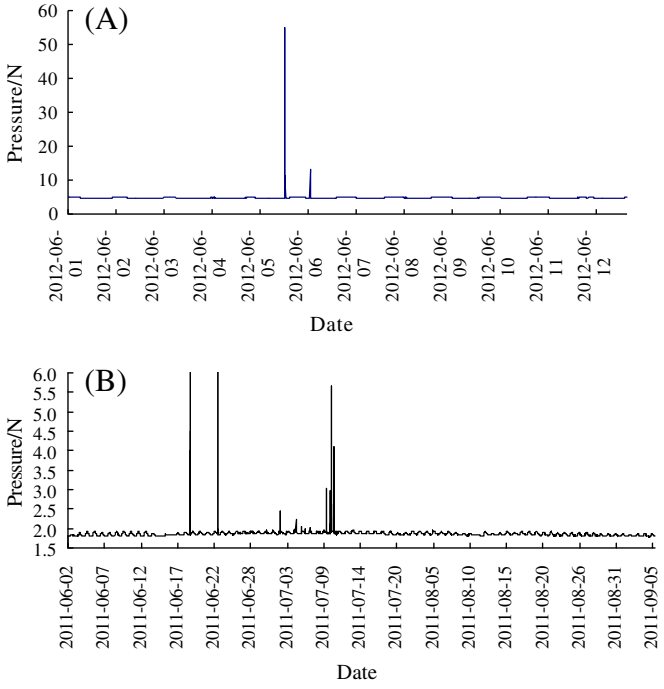

Fig. 8. The abrupt changes in pressure after (A) 15 mm and (B) 48.1 mm of rainfall.

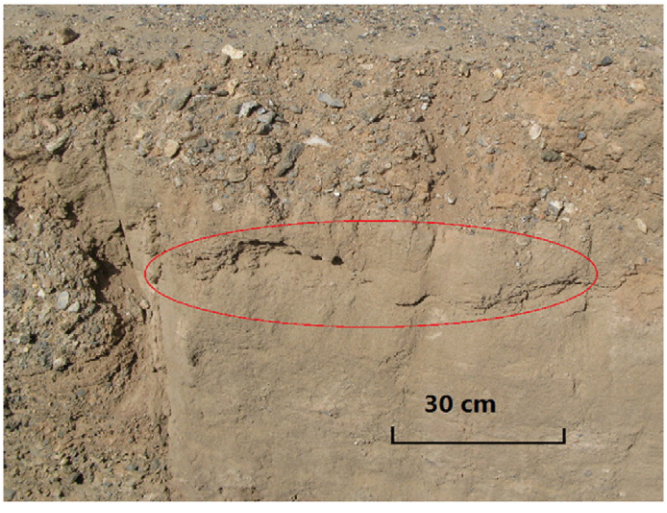

Fig. 9. Superimposed layers (highlighted using a ellipse) in the fissure surface affected by many small rainfalls.

exposure to the long-term drought conditions prevalent since the last glacier.

Thirdly, their distribution regions are different. Arid sand wedges form as the result of long periods of drought and are closely related to precipitation. The Gobi surface preservation time determines the sand-wedges' degree of development. The larger sand wedges in the land surface have experienced a longer time in an extra-arid environment. So theoretically, as long as the soil experiences alternating dry and wet conditions it should form fractures, undergo wet expansion, and form arid sand wedges. Therefore, even in semihumid areas sand wedges should form provided the soil has a short-term dry status. However, if we consider that once the precipitation increases to a certain threshold, such as happens in semihumid areas, a runoff would form to erode the land surface or the flood would leave deposits that cover the land surface. This cannot form or maintain a sand wedge. According to the arid sand-wedge formation mechanism, only if the surface is exposed for a long time, experiences temperature variations and alternate periods of wet and dry, and is protected from erosion (or the erosion speed is less than formation speed) can a sand wedge be formed and maintained. Therefore, for this reason, arid sand wedges are inevitably distributed in arid or semiarid areas, particularly in extra-arid areas. In contrast, frozen sand wedges are distributed in the wet chilling areas such as the permafrost tundra and periglacial edges.

In the Hexi Corridor, arid sand wedges are distributed in relatively flat places (Wang et al., 2003). Most of them have been found in high terraces, mesas, or hillock ground. Just as in the high mesa platform of Mogao and Yangguan (which avoid erosion and flood deposition), the land here has had a long time to develop and safely preserve the sand wedges. This is why in some places the sand wedges are smaller in size or even nonexistent.

Seeing as arid sand wedges can form in extra-arid areas by the mechanism we are studying, for sand wedges in low latitudes we need to conduct further studies to decide whether these wedges are relicts of a cold climate. They are a problem if they are only based on the freezing–thawing mechanism used to reconstruct paleoclimate. Making a Snowball Earth hypothesis or a theory of high obliquity of the Earth's ecliptic is also not reliable based on sand wedges found in places near to the equator. Therefore, the discovery of the new arid sand-wedge formation mechanism has removed the constraint of a single formation mechanism based on freezing–thawing. It provides a new concept in the study of sand wedges in low latitudes on the Earth, and it is also significant in regard to research on the polygon structures on Mars and other planets.

6. Conclusions

Sand wedges are widely distributed in the extra-arid Gobi area. We have revealed their formation mechanism by excavating some arid sand wedges, analyzing their salinity and moisture content, monitoring the movement of polygon matrices, and by simulating a rainfall experiment. An arid sand wedge is formed by cycles of wet expansion and dry shrinking. The salinity is the main bonding material that consolidates the gravels and is important for arid sand-wedge formation. The rainfall also plays a key role in the process. The fact that the sand wedge is gradually formed over a very long time means that it contains very rich historical information. It is a unique arid landmark and has important value in the reconstruction of the paleoclimate and research on polygon structures on other planets. This research also has important implications for protection of the relics in the Mogao Grottoes.

Acknowledgments

This work is supported by the National Natural Science Foundation of China (no. 41363009), a project of the Dunhuang Academy (no. 201306), and the Natural Science Foundation of Gansu Province (no. 1308RJZF290). We are grateful to Yulei He from the Reception Department of the Dunhuang Academy for her help with translation. The editor Richard A. Marston and the three anonymous reviewers who provided valuable comments and suggestions were also appreciated.

Appendix A. Supplementary data

Supplementary data to this article can be found online at http://dx.doi.org/10.1016/j.geomorph.2013.12.028.

References

Adam, C.M., James, B.K., Alison, M.A., 2002. Neoproterozoic sand wedges: crack formation in frozen soils under diurnal forcing during a snowball Earth. Earth Planet. Sci. Lett. 204, 1–15.
Andersland, O., Ladanyi, B., 1994. An Introduction to Frozen Ground. Chapman and Hall, London.
Bateman, M.D., Murton, J.B., Boulter, C., 2010. The source of D_e variability in periglacial sand wedges: depositional processes versus measurement issues. Quat. Geochronol. 5, 250–256.
Black, R., 1976. Periglacial features indicative of permafrost: ice and soil wedges. Quat. Res. 6, 3–26.
Bockheim, J.G., 2007. Soil processes and development rates in the Quartermain Mountains, upper Taylor Glacier region, Antarctica. Geogr. Ann. 89 (3), 153–165.
Bockheim, J.G., Kurz, M.D., Soule, S.A., Burke, A., 2009a. Genesis of sand-wedge polygons in Beacon Valley, Antarctica. Permafr. Periglac. Process. 20, 295–308.
Bockheim, J., Coronato, A., Rabassa, J., Ercolano, B., Ponce, J., 2009b. Relict sand wedges in southern Patagonia and their stratigraphic and paleo-environmental significance. Quat. Sci. Rev. 28, 1188–1199.
Brook, E.J., Kurz, M.D., Ackert, R.J., Denton, G.H., Brown, E.T., Raisbeck, G.M., Yiou, E., 1993. Chronology of Taylor Glacier advances in Arena Valley, Antarctica, using in situ cosmogenic ^{3}He and ^{10}Be. Quat. Res. 39, 11–23.
Buczkowski, D.L., Seelos, K.D., Cooke, M.L., 2012. Giant polygons and circular graben in western Utopia basin, Mars: exploring possible formation mechanisms. J. Geophys. Res. Planets 117 (E8) (1991–2012).
Chang, X.L., Jing, H.J., He, R.X., 2011. Formation and environmental evolution of sand wedges on the Tianshuihai north lakeshore in the western Kunlun mountains. Quat. Sci. 31, 112–119.
Cherykov, V.Y., 2000. Using surface crack spacing to predict crack network geometry in swelling soils. Soil Sci. Soc. Am. J. 64, 1918–1921.
Cui, Z.J., Song, C.Q., 1992. Holocene periglacial process and environmental changes in the Daqingshan Mountains, Inner Mongolia, China. J. Glaciol. Geocryol. 14, 325–331 (in Chinese).
Cui, Z.J., Yang, J.Q., Zhao, L., 2004. Discovery of extensive distributed ice wedges in Erdos Plateau: the permafrost boundary and environment in the North of China during the past 20 ka. Chin. Sci. Bull. 49, 1304–1310.
Deynoux, M., 1982. Periglacial polygonal structures and sand wedges in the late Precambrian glacial formations of the Taoudeni Basin in Adrar of Mauretania (West Africa). Palaeogeogr. Palaeoclimatol. Palaeoecol. 39, 55–70.
Dong, G.R., Gao, S.Y., Li, B.S., 1985. Paleoperiglacial phenomena and its significance in climatic stratigraphy in the Ordos Plateau during the Late Pleistocene. Geogr. Res. 4, 1–12 (in Chinese).
Dong, G.R., Li, B.S., Gao, S.Y., 1996. The relation of paleo-periglacial phenomena and the wind blow sand or loess in Ordos Plateau since late Pleistocene. Memoirs of Institute of Desert, Academia Sinica, Lanzhou, China, vol. 3. Science Press, Beijing 8–25.
French, H.M., Demitroff, M., Forman, S.L., 2003. Evidence for late-Pleistocene permafrost in the New Jersey Pine Barrens (latitude 39° N), eastern USA. Permafr. Periglac. Process. 14, 259–274.
Guo, D.X., 1979. Sandy wedges in the Qinghai Xizang Plateau. J. Glaciol. Geocryol. 1, 51–73 (in Chinese).
Guo, D.X., Li, Z.F., 1981. Preliminary approach to the history and age of permafrost in Northeast China. J. Glaciol. Geocryol. 3, 1–16 (in Chinese).
Guo, Q.L., Wang, X.D., Zhang, H.Y., Li, Z.X., Yang, S.L., 2009. Damage and conservation of the high cliff on the Northern area of Dunhuang Mogao Grottoes, China. Landslides 6, 89–100.
Hallarire, V., 1989. A 3-dimensional description of cracks network on clayey soils using image analysis and a structural model. Acta Stereol. 8, 301–306.
Huang, C.Q., Shao, M.A., 2008. Experimental study on soil shrinking and swelling characteristics during the alternative drying and wetting processes. Chin. J. Soil Sci. 39, 1243–1247.
Kaplar, C., 1963. Laboratory determination of the dynamic module of frozen soils and of ice. Proceedings, Permafrost International Conference Publication, 1287, pp. 293–301.
Kovács, J., Fábián, S.A., Schweitzer, F., Varga, G., 2007. A relict sand wedge polygon site in north central Hungary. Permafr. Periglac. Process. 18, 379–384.
Lachenbruch, A.H., 1962. Mechanics of thermal contraction cracks and ice-wedge polygons in permafrost. Geol. Soc. Am. 70, 69.
Levy, J.S., Head, J.W., Marchant, D.R., 2009. Cold and dry processes in the Martian Arctic: geomorphic observations at the Phoenix landing site and comparisons with terrestrial cold desert landforms. Geophys. Res. Lett. 36 (21), L21203.
Li, H., Yang, H., 2000. Experimental investigations of fracture toughness of frozen soils. J. Cold Reg. Eng. 14, 43–49 (in Chinese).
Li, H.S., Wang, W.F., Zhan, H.T., 2010a. New judgement on the source of soil water in extremely dry zone. Acta Ecol. Sin. 30, 1–7.

Li, H.S., Wang, W.F., Zhang, G.B., Zhao, L.Y., 2010b. Measurement of deep buried phreatic water evaporation in extremely arid area. Acta Ecol. Sin. 30, 6798–6803 (in Chinese).
Li, H.S., Wang, W.F., Zhang, G.B., Zhang, Z.M., Wang, X.W., 2011. GSPAC water movement by Greenhouse method in the extremely dry area. J. Arid. Land 3, 141–149.
Liang, F.X., Cheng, G.D., 1984. Polygon veins along the Qinghai Xizang highway. J. Glaciol. Geocryol. 6, 49–59 (in Chinese).
Liu, D.S., 2009. Loess and Arid Environment. Anhui Science and Technology Press, Hefei 58–90.
Lu, D.Q., Shao, M.A., 2003. A review of soil shrinkage characteristics. Chin. J. Soil Sci. 34, 225–228.
Luo, Y.H., Fu, X.D., 2007. The research of displacement of sandy soil humidifying. Shanxi Archit. 33, 115–117 (in Chinese).
Macphail, R., Goldberg, P., 2010. Archaeological materials. In: Stoops, G., Marcelino, V., Mees, F. (Eds.), Interpretation of Micromorphological Features of Soils and Regoliths. Elsevier, Amsterdam, pp. 589–622.
Marchant, D.R., Lewis, A.R., Phillips, W.M., Moore, E.J., Souchez, R.A., Denton, G.H., Sugden, D.E., Potter, N.J., Landis, G.P., 2002. Formation of patterned ground and sublimation till over Miocene glacier ice in Beacon Valley, southern Victoria Land, Antarctica. Geol. Soc. Am. Bull. 114, 718–730.
Mears, B., 1981. Periglacial wedges and the Late Pleistocene environment of Wyoming intermountain basin. Quat. Res. 15, 171–198.
Mellon, M., 1997. Small-scale polygonal features on Mars: seasonal thermal contraction cracks in permafrost. J. Geophys. Res. — Atmos. 102, 25617–25628.
Murton, J.B., 1996. Morphology and paleoenvironmental significance of Quaternary sand veins, sand wedges, and composite wedges, Tuktoyaktuk coastlands, western arctic Canada. J. Sediment. Res. 66, 17–25.
Murton, J.B., Bateman, M.D., 2007. Syngenetic sand veins and anti-syngenetic sand wedges, Tuktoyaktuk coastlands, western arctic Canada. Permafr. Periglac. Process. 18, 37–47.
Murton, J.B., Worsley, P., Gozdzik, J., 2000. Sand veins and wedges in cold aeolian environments. Quat. Sci. Rev. 19, 899–922.
Pan, B.T., Chen, F.H., 1997. Permafrost evolution in the Northeastern Qinghai–Tibetan Plateau during the last 150 000 years. J. Glaciol. Geocryol. 19, 124–132.
Paul, F.W., 1976. 'Random' hunting and the composition of faunal samples from archaeological excavations: a modern example from New Zealand. J. Archaeol. Sci. 3, 321–328.
Qin, Y.H., 2011. General Physics Course, Thermology. Higher Education Press, Beijing.
Rist, M., Sammonds, P., Murrell, S., Meredith, P., Doake, C., Oerter, H., Matsuki, K., 1999. Experimental and theoretical fracture mechanics applied to Antarctic ice fracture and surface crevassing. J. Geophys. Res. — Atmos. 104, 2973–2987.
Shao, M.A., Lu, D.Q., 2003. The study of soil contraction indicatrix. Acta Pedol. Sin. 40, 471–474 (in Chinese).
Shao, M.A., Lu, D.Q., Fu, X.L., 2007. Quantitative relationship between mass water content, pressure head and bulk density in determination of soil water retention characteristic I. Packed soils. Acta Pedol. Sin. 44, 1003–1009 (in Chinese).
Shi, Y.F., Zheng, B.X., Yao, T.D., 1997. Glaciers and environment during the Last Glacial Maximum on the Tibetan Plateau. J. Glaciol. Geocryol. 19, 97–113 (in Chinese).
Siebert, N., Kargel, J., 2001. Small-scale Martian polygonal terrain: implications for liquid surface water. Geophys. Res. Lett. 28, 899–902.
Singleton, A.C., Osinski, G.R., Samson, C., Williamson, M.-C., Holladay, S., 2010. Electromagnetic characterization of polar ice-wedge polygons: implications for periglacial studies on Mars and Earth. Planet. Space Sci. 58 (4), 472–481.
Sohl, L.E., Christie-Blick, N., Kent, D.V., 1999. Paleomagnetic polarity reversals in Marinoan (ca. 600 Ma) glacial deposits of Australia: implications for the duration of low-latitude glaciation in Neoproterozoic time. Geol. Soc. Am. Bull. 111, 1120–1139.
Wang, B.L., French, H.M., 1991. Soil wedge and ice wedge pseudomorphs and their paleoclimatic implications. J. Glaciol. Geocryol. 13, 67–76 (in Chinese).
Wang, N.A., Wang, T., Shi, Z.T., 2001. The discovery of sand wedges of the last glaciation in the Hexi Corridor and its paleoclimatic significance. J. Glaciol. Geocryol. 23, 46–50 (in Chinese).
Wang, N.A., Zhao, Q., Li, J.J., Hu, G., Cheng, H.Y., 2003. The sand wedges of the last ice age in the Hexi Corridor, China, paleoclimatic interpretation. Geomorphology 51, 313–320.
Washburn, A.L., 1979. Geocryology. Edward Arnold, London (406 pp.).
Williams, G.E., 1975. Late Precambrian glacial climate and the Earth's obliquity. Geol. Mag. 112, 441–465.
Williams, G.E., 2001. The paradox of Proterozoic glaciation at sea level and strong seasonality near the paleoequator: evidence and implications. Geol. Soc. Aust. 65, 108–112.
Williams, G.E., Tonkin, D.G., 1985. Periglacial structures and paleoclimatic significance of a late Precambrian block field in the Cattle Grid copper mine, Mount Gunson, South Australia. Aust. J. Earth Sci. 32, 287–300.
Wu, J.C., Sheng, Y., Yu, H., 2007. Permafrost in the middle-east section of Qilian Mountains (I): distribution of permafrost. J. Glaciol. Geocryol. 29, 418–425.
Xiong, D.H., Zhou, H.Y., Du, C.J., 2006. A review on the study of soil cracking. Soils 38, 249–255 (in Chinese).
Yang, J.C., Sun, J.Z., Li, S.D., 1983. Fossil ice wedges and Late Pleistocene environment in Datong Basin, Shanxi Province. Sci. Geogr. Sin. 3, 339–344.
Zhu, X.Y., Qian, X.X., 2005. Groundwater Hydrology. China Environmental Science Press, Beijing (14–16 pp.).